The Egyptian Journal of Hospital Medicine (October 2022) Vol. 89 (2), Page 7419- 7428

Performance of Pathognomonic Magnetic Resonance Imaging Findings for Diagnosis of Triple Negative Breast Cancers

Marwa Elsayed Abd Elhamed*, Rabab M. Abdelhay, Ghada Adel AbdelHamid, Ahmed Gamil Ibrahim Abd El Megid

Department of Radiodiagnosis, Faculty of Medicine, Zagazig University, Sharkia, Egypt

***Corresponding author:** Marwa Elsayed Abd Elhamed, **Mobile:** (+20)01114473406, **E-Mail:** dr.meroelsayed34@gmail.com

ABSTRACT

Background: Triple Negative Breast Cancer (TNBC) has the worst prognosis of any subtype of the disease because of tumor heterogeneity and a chronic lack of other effective treatment lines. To improve the low survival rate, early identification is the key.

Objective: Our study aimed to determine the accuracy of Dynamic Contrast-Enhanced Magnetic Resonance Imaging (DCE-MRI) in differentiating TNBC from other Non-Triple Negative Breast Cancer (NTNBC) subtypes using pathological examination as the gold standard.

Subjects and procedures Retrospective study was conducted at the Radio-diagnosis, Oncology, and Surgery departments of Meet Ghamr Oncology center, enrolling 68 female patients with pathologically proven 83 malignant breast lesions of different immunochemistry subtypes, consisting of TNBC (22 patients/29 lesions) and NTNBC (46 patients /54 lesions). Every patient received both conventional and (DCE) MRI scans, which are compared to histopathological and immune-chemistry analyses.

Results: TNBC and NTNBC subtypes groups differed significantly ($p<0.05$) in terms of the tumor's size, shape, Apparent Diffusion Coefficient (ADC) value, enhancement shape and distribution, and specific criteria like central necrosis and peritumoral high T2 Weighted Image (T2WI) signal. There was a highly significant difference ($p<0.001$) between the two groups in terms of (Patient age, histologic grade, tumor margin, lesion-high T2W signal, and enhancement pattern). Validity values for differentiating between TNBC and NTNBC using combined DCE-MRI and MRI-Specific criteria were (100%, 91.49%, 87.1%, and 100%) as opposed to (88.89%, 97.87%, 96%, and 93.9%)

Conclusions: The results of our study demonstrated the possibility of MRI-based imaging criteria for more accurate prediction and differentiation of TNBC from other subtypes.

Keywords: Triple-negative breast cancer, DCE-MRI, NTNBC.

INTRODUCTION

In 2005, a subtype of breast cancer known as triple negative (TNBC) was discovered and was distinguished by the absence of overexpression of the Human Epidermal growth factor Receptor 2 (HER2) and the lack of expression of the estrogen and progesterone receptors [(1)]. Ten to twenty percent of breast cancers are TNBC, and these cases are more deadly and more likely to recur than those with other types of breast cancer because there is currently no effective targeted therapy for them [(2)].

Chemotherapy is the only proven clinically effective therapy for TNBC. To properly plan treatment and predict how patients will respond to neoadjuvant chemotherapy (NCT), which is given before breast cancer surgery, it is crucial to distinguish TNBC from non-TNBC (NTNBC) patients as soon as possible [(3)].

Currently, immunohistochemical analysis, in which tumor tissue samples are obtained through biopsy is required for breast cancer molecular subtyping. Restrictions are placed on data collection and processing due to the invasive nature of this technology. In contrast, imaging is noninvasive and can disclose the broad features of a tumor, opening the door to studies of molecular distinctions between subtypes and dynamic evaluations of therapy efficacy as well as their outcomes [(3)]. Mammographic features indicative of breast cancer are absent in TNBC, including an unusual mass shape, spiculated margins, and associated suspicious calcifications. Because of this, mammography is not always the best option for a primary diagnostic evaluation. Despite ultrasound's superior sensitivity compared to other imaging modalities, the presence of benign characteristics in 21% to 41% of TNBC lesions may impair the modality's capabilities to diagnose these tumors [(4)].

It can also be diagnosed using DCE-MRI, which has various characteristics associated with the aggressive malignant behavior of triple-negative malignancy. The most accurate diagnostic imaging method is DCE-MRI because it detects malignant MRI characteristics that may not be seen with mammography or ultrasound. The specific criteria, such as central tumor necrosis and peritumoral high T2WI signal intensity, which are recently linked to triple-negative cancer, however, poorly understood [(5)].

So, using pathological examination as the gold standard, our study sought to determine the precision of MRI-based specific criteria in differentiating indeterminate TNBC from other subtypes.

PATIENTS AND METHODS

From March 2022 to July 2022, our retrospective study was carried out at the Meet Ghamr Oncology Center's Department of Oncology, Surgery, and Radiodiagnosis. In our study, 68 female patients with 83 newly pathologically confirmed breast cancer were enrolled. Based on immunochemistry data, all lesions

Received: 15/07/2022
Accepted: 18/09/2022

were divided into two groups: 22 patients/29 TNBC and 46 patients/54 NTNBC.

Ethical consent:

The Institutional Review Board of the School of Medicine at Zagazig University (#10138) gave their approval to the study, and all patients gave their written informed permission. The experiment followed the ethical guidelines laid out in the Declaration of Helsinki by the World Medical Association. In-depth clinical evaluations, pathological analyses, conventional MRIs, and post-contrast dynamic MRIs are all performed in every case.

Inclusion criteria: Female patients with pathologically and immunochemically proven breast cancer lesions meet the inclusion criteria.

Exclusion criteria: Patients who have undergone surgery or have received neo-adjuvant chemotherapy (NCT), also patients with breast implants and for whom histopathology or immunochemistry results are not yet available.

Data Collection:

Patient names, ages, clinical presentations, family histories, and histopathological diagnoses were collected, and then a BI-RADS category was assigned to each patient based on the lexicon used by BI-RADS.

MRI technique:

Breast MRI was performed on all cases utilizing 1.5 Tesla technology (Siemens, Aera 1.5 Tesla). Each subject was examined using specialized bilateral breast surface coils while lying prone; the duration of the research was between 30 and 45 minutes. Premenopausal women were imaged from the seventh to the fourteenth day of their menstrual cycle, with the patient being asked to remain still throughout the procedure.

I- **Standard MR protocol was:** Common MR protocols involved acquiring an axial non-fat saturated TIWI using FSE, with the following settings: (TR 450 ms, TE 14 ms, slice thickness 3 mm, field of view (FOV) 300-360 mm, matrix 512x512. Acquiring turbo spin echo (TR/TE = 120/4.9 msec) axial T2-weighted images were used to create the STIR sequence. T1- and T2-weighted pulse sequence with fat saturation before contrast, set to the following values: Slice thickness was 3-4 mm, field of view (FOV) was 300- 360 mm, inversion time (TI) was 150 ms, and the matrix size was 512 x 512.

II- **Diffusion-weighted Image:** A DWI examination took place for two minutes before the injection of contrast using single-shot echo planner imaging at b values (0,300,1000 s/mm2), TR/TE:1800/75, slice thickness:3 mm without a gap, and FOV:350 mm. The ADC value was computed when the ADC Map was completed. By combining the study of the tumor shape and the visual diffusion signal pattern in the DWI and ADC maps with a high b value, qualitative evaluations were carried out. The (ADC) measurements gave quantifiable data. Lesions with an ADC value equal to or below 1 x 10-3 mm2 /s and a high signal on high b values series were judged confined.

III- **Dynamic study:** To suppress fat, all dynamic investigations were carried out in the axial plane utilizing pulses that were saturated in fat. The FLASH 3D GRE-T1W1 sequence was used, with the following parameters: TR 4-8 ms, TE 2 ms, flip angle 20-25 degrees, slice thickness 2 mm without an interslice gap, field of view (FOV) 300-360 mm, and a matrix of 512 x 512. In the dynamic study, which consists of one pre-contrast and five post-contrast series, there is a 20-second break between the pre-contrast and post-contrast tests.

Post. processing:

Positive features of the picture were emphasized using subtraction during post-processing. Using a time/signal intensity curve for quantitative analysis, maximum intensity projection (MIP) was used to display the geographical distribution of illness in the breast in relation to the skin, nipple, chest wall, and main blood arteries.

Morphological characteristics:

The two types of enhancing lesions were mass and non-mass enhancement.

I-Mass enhancement:

A mass lesion takes up space in three dimensions. Shape (oval, round, irregular), edge (smooth, irregular, spiculated), and internal enhancing characteristics of the masses are numerous (homogenous, heterogenous, rim enhancement).

II-Non-mass enhancement:

Internal enhancement properties (homogenous, heterogeneous, and ring) and distribution pattern (linear enhancement, segmental enhancement, regional enhancement).

Evaluation of the kinetic enhancement curve:

The time/signal intensity curve led to the classification of three pattern types, I benign (persistent), II borderline (plateau), and III malignant (washout).

Figures 1,2 and 3 show demonstrative cases.

Standard of reference

All patients underwent a core needle biopsy using a 14 Gauge automated biopsy gun or semi-automated biopsy gun, all patients underwent histopathological and immunochemistry examination, and 32 patients underwent surgery (excisional biopsy including the 32 cases with non-mass-like enhancement on MRI). As a benchmark, the results of the combined histopathological and immunochemistry tests had been used.

Statistical analysis

SPSS software was used to gather and analyze the data (IBM, Version 20.0). The terms mean, range, percentage, and standard deviation were employed to describe quantitative data (IQR). The Chi-square and Student's t-tests were used for categorical variables. A two-tailed significance threshold was used to determine each p-value. Validity measurements (sensitivity, specificity, NPV, and PPV) were also calculated if the probability was less than 0.05 and the significance level was less than 0.001. These values were deemed as statistically significant and highly statistically significant, respectively.

RESULTS

Our current study enrolled 68 female patients with 83 pathologically proven malignant breast lesions, based on immunochemistry analysis, malignant lesions were distributed into TNBC subtype group (22 patients /29 lesions) and NTNBC subtype group (46 patients /54 lesions)

Table 1: Revealed statistical significance in **patients' age**, mean age is 41±1.3 for the TNBC group and 52±2.4 for the NTNBC group, with a significant in-between difference, P<0.0001.

The palpable mass was the **most common complaint** in patients with TNBC 21/22 (95.5%), however, the asymptomatic patients who came for screening were mostly belonged to NTNBC 31/46(67.4%), with a significant in-between difference with p=0.011105. Patients with a **positive family history** are the majority of both groups, 12/22(54.5%) and 17/46(36.9%) for TNBC and NTNBC groups respectively. As regards the **BIRADS lexicons**. BIRAD IV is the most category in both study groups, 16/29 (55.2%) for the TNBC group and 34/54(62.9%) for the NTNBC group.

Histologic grading revealed that 16/29 (55.2%) of the TNBC were of a histologic grade III, compared with 34/54(62.9%) of the NTNBC (p < 0.000133). **By histopathological analysis**, we noticed that most tumors in both groups were invasive ductal carcinomas (IDC). Of the 17/29(58.6%) TN breast cancer, 9/29 (31.03%) were invasive intralobular carcinoma (ILC), and there were 3/29(10.3) mixed types. Of the NTNBC, 27/54(50 %) were IDC, and there were 22/54(40.7%) ILC and 5/54(9.3%) mixed type, with no significant in-between difference (p value=0.68267).

Table (1): Comparison between the two studied groups according to Clinic-pathologic characteristics

Clinical Criteria (n=68)	TNBC(n=22)	NTBNC(n=46)	Test	P-value
Age				
Range	33-52	36-73	t	<0.0001
Mean	41±1.3	52±2.4	20.0825	
Complaint				
Palpable mass	21(95.5%)	13(28.3%)		
Pain	8(36.4%)	22(47.8%)		
Nipple discharge	4(18.2%)	11(23.9%)	X^2	0.011105
screening	15(68.2%)	31(67.4%)	11.118	
Family History				
Yes	12(54.5%)	17(36.9%)	X^2	0.170065
No	10(45.5%)	29(63 %)	1.8824	
Pathologic Criteria (n=83)	**TNBC(n=29)**	**NTNBC (n=54)**	**Test**	**P-value**
BIRADS Lexicon				
III	8(27.6%)	11(20.4%)		
IV	16(55.2%)	34(62.9%)	X^2	0.732371
V	5(17.2%)	9(16.7%)	0.6229	
Histologic grade				
I	2(6.9%)	14(25.9%)	X^2	
II	10(34.5%)	32(59.3%)	17.8534	0.000133
III	17(58.6%)	8(14.8%)		
Histologic subtype				
IDC	17(58.6%)	27(50%)		
ILC	9(31.03%)	22(40.7%)	X^2	0.68267
Mixed	3(10.3%)	5(9.3%)	0.7635	

t: Sudent't test**, $X^{2:}$** Chi-square test

Table 2: Relating to the MRI results, tumors were bilateral in 3 out of 29 cases (10.34%) in TNBC and 2 out of 54 cases (3.7%), and multifocal in 2 out of 29 cases (6.9%) in TNBC and 1 out of 54 cases (2.9%), with a p-value of 0.850436.

TNBC subtype was observed to have a larger tumor size (>2 cm) in (21/29, 72.4%) compared to (23/54, 42.6%) with a significant difference. (P = 0.0009449). TNBC subtypes with mass-like amplification tended to have oval shapes (12/29, 41.4%), whereas NTNBC subtypes tended to have irregular shapes (39/54, 72.2%), with a P value of 0.00082. While NTNBC margins were generally spiculated (32/54 59.3%), TNBC margins were smooth 21/29(72.4%), with a P value of 0.00001. High T2 signal intensity within tumors relative to normal breast tissue was seen on unenhanced fat-suppressed T2-weighted images in 23/29 (79.3%) of TNBC subtype cases and 15/54 (27.8%) of NTNBC cases (p<0.0001).

As regards the **diffusion** ،restricted diffusion was predominant at the TNBC subtype was 19/29(65.5%) versus 17/54 (31.5%) for NTNBC with a significant difference, p=0.002853. Differences in ADC levels between the two tumors types were statistically significant (P= 0.0412), the mean ADC value of TNBC ranged between (0.723–1.709), mean ±SD=1.034 ± 0.201swhich was higher than that of NTNBC subtypes which ranged (0.891 ± 0.202), mean ± SD(0.312–2.230). Concerning **the axillary state,** the enlarged axillary lymph nodes did not differ significantly between the studied groups.

Table (2): Comparison between the two studied groups according to MRI morphologic findings

MRI findings Morphologic CCC	TNBC (n=29) n(%)	NTNBC (n=54) n(%)	Test	P-value
Bilaterality	3(10.34%)	2(3.7%)	X^2	
	2(6.9%)	1(1.9%)	0.0356	0.850436
Multiplicity				
Size				
>2 cm	21(72.4%)	23(42.6%)	X^2	0.0009449
<2 cm	8(27.6%)	31(57.4%)	6.736	
Shape				
Oval	12(41.4%)	4(7.41%)	X^2	
Round	9(31.03%)	11(20.4%)	18.8245	0.00082
Irregular	8(27.6%)	39(72.2%)		
Margins				
Spiculated	3(10.3%)	15(27.8%)	X^2	
Irregular	5(17.2%)	32(59.3%)	29.8838	<0.00001
Smooth	21(72.4%)	7(12.9%)		
High T2 SI				
Yes	23(79.3%)	15(27.8%)	X^2	<0.00001
No	6(20.7%)	39(72.22%)	20.1854	
Restricted DWI				
Yes	19(65.5%)	17(31.5%)	X^2	0.002853
No	10(34.5%)	37(68.5%)	8.899	
ADC value ($\times 10^{-3}$ mm^2/s)	1.034 ± 0.201 (0.723–1.709)	0.891 ± 0.202 (0.312–2.230)	t 2.0750	0.0412
Axillary state			X^2	
+ve	15(51.7%)	22(40.7%)	0.9213	0.337144
-ve	14(48.3%)	32(59.3%)		

Table 3: Qualitative and quantitative DCE-MRI findings: Twenty-one out of twenty-nine (72.4%) TNBC subtype lesions exhibited mass-like enhancement versus Most NTNBC lesions (39/54, 72.2%) exhibited non-mass-like enhancement, with segmental non-mass enhancement more at TNBC subtype (6/29,20.7%) versus regional non-mass enhancement common at NTNBC subtype (27/54, 50%), with a significant difference, p=0.00091. Post-contrast DCE-MRI images revealed that rim enhancement was the most common kind of internal enhancement in TNBCs (17/29, 58.6%), while heterogeneous internal enhancement was at NTNBC subtype (37/54, 68.5%), with statistically significant difference (p<0.00001). Dynamic curve study revealed type III (wash-out) and type II (plateau) curves in 16(55.2%), and 10(34.5%) of TNBC compared to (35/54, 64.8 %) & (13/54, 24.1%) respectively in NTNBC subtypes, with no statistically significant difference (P= 0.596496).

Table (3): Comparison between the two studied groups according to quantitative and qualitative DCE-MRI findings

MRI Findings	TNBC (n=29) n(%)	NTNBC (n=54) n (%)	X^2	P-value
Enhancement				
Mass	21(72.4%)	15(27.8%)		
Nonmass	8(27.6%)	39(72.2%)		
Distribution				
Segmental	6(20.7%)	12(22.2%)	15.3052	0.00091
Regional	2(6.9%)	27(50%)		
Patterns				
Homogeneous	4(13.8%)	14(25.9%)	29.1598	<0.00001
Heterogeneous	8(27.6%)	37(68.5%)		
Rim	17(58.6%)	3(5.6%)		
Kinetic study				
Type I persistent	3 (10.3%)	6(11.1%)		
Type II plateau	10(34.5%)	13(24.1%)	1.0334	0.596496
Type III washout	16(55.2%)	35 (64.8%)		

Table 4: There was a statistically significant difference between the two studied groups as regards the **specific MRI criteria** including perilesional edema & central necrosis found in (15/29,51.7%), (11/29,37.9%) respectively of TNBCs versus (11/54,20.4%), (4/54,7.4%) respectively of NTNBC, with statistic significant difference (p=<0.05).

Table (4): Comparison between the two studied groups according to specific criteria (peri-lesional edema and intralesional necrosis)

Specific criteria	TNBC (n=29) n(%)	NTNBC (n=54) n(%)	X^2	P-value
Peri-lesional edema				
Yes	15(51.7%)	11 (20.4%)	8.6219	0.003322
No	14(48.3%)	43(79.6%)		
Central necrosis				
Present	11(37.9%)	4 (7.4%)	11.8725	0.00057
Absent	18(62.07%)	50(92.6%)		

Table 5: Validity (sensitivity%, specificity%, PPV%, and NPP%) for combined DCE-MRI and MRI-Specific criteria in differentiating between TNBC & NTNBC subtypes, where sensitivity=100%, specificity= 91.49%, PPV= 87.1% and NPP=100% for TNBC subtype, while sensitivity=88.89%, specificity= 97.87%, PPV=96% and NPP=93.9% for NTNBC subtypes.

Table (5): Validity of combined dynamic contrast-enhanced MRI and specific MRI criteria in differentiating TNBC from NTBC subtypes

Subtypes	Sensitivity%	Specificity%	PPV%	NPP%
TNBC	100	91.49	87.1	100
NTNBC	88.89	97.87	96.0	93.9

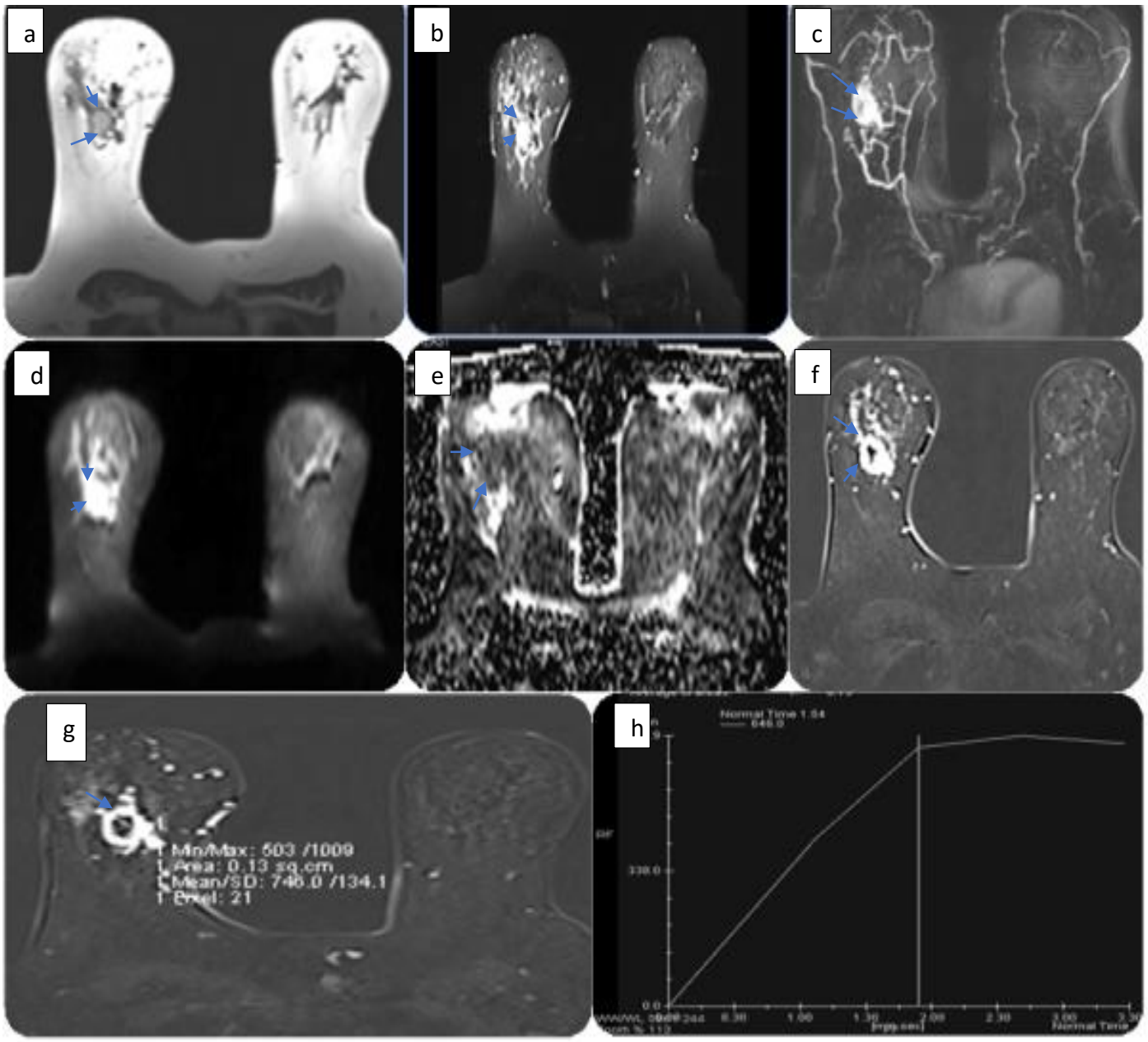

Fig. (l): Female patient 37 years old age. presented by Rt palpable non-painful breast mass and bloody nipple discharge. MRI axial cuts a) T2WI. b)STIR. c) MIP. d)DWI. e) ADC map. f).g) DCE-MRI subtracted post-con hast T1WI. h) dynamic study. (arrows) revealed Rt breast 12 O'clock well-circumscribed round-shaped mass lesion measuring 26 x 28 mm. with central necrosis, with intra- and peri-lesional high T2. signal. restricted diffusion, postcontrast rim enhancement, and type II plateau (borderline) curve, pathological proved TNBC, IDC.

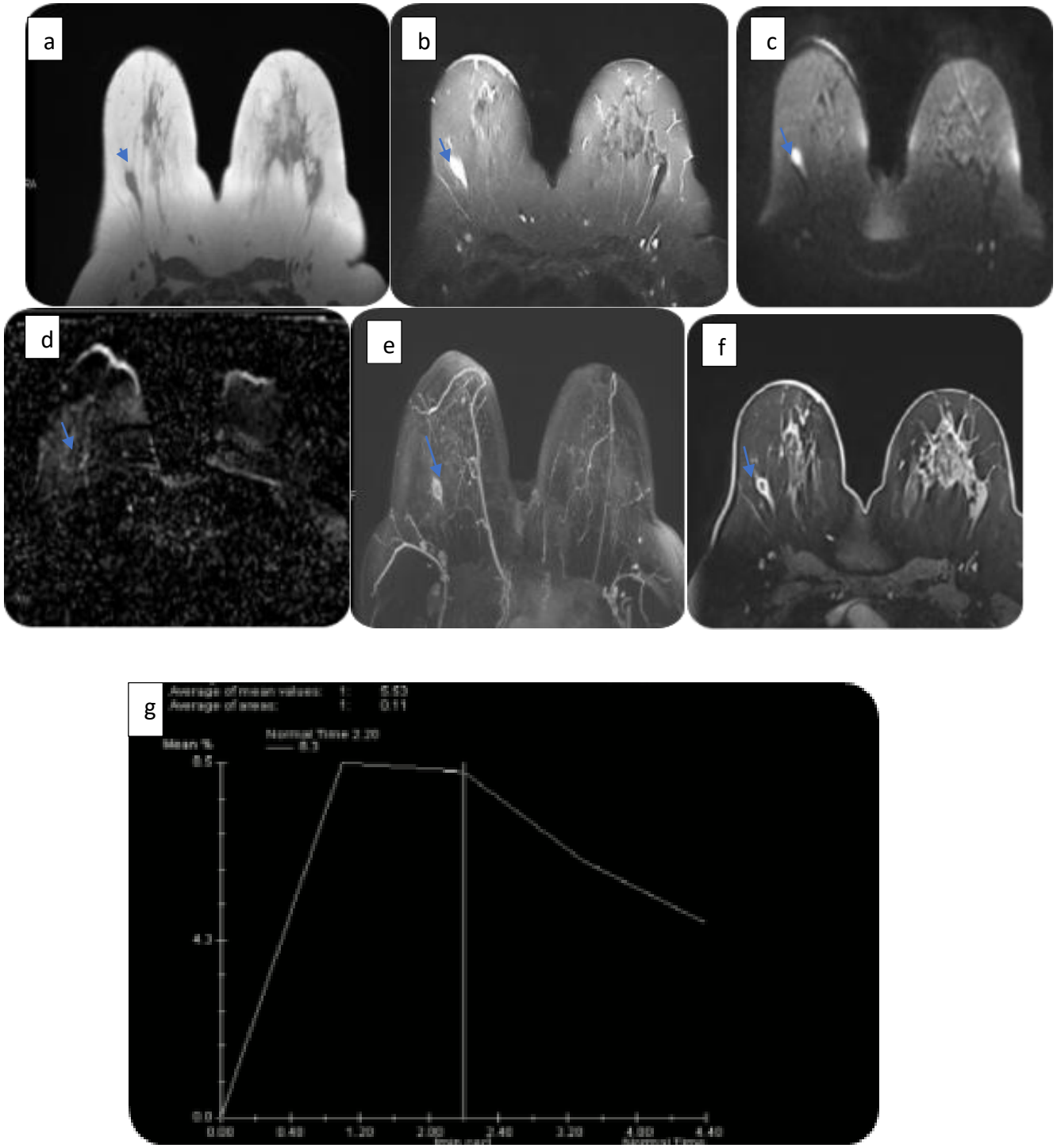

Fig. (2): Female patient 43 years old age, came for screening, axial MR cuts a)T2WI, b)STIR,c)DWI, d)ADC, e)MIP, f)DCE-MRI based postcontrast subtracted images & g)dynamic curve, (arrows) revealed Rt breast upper outer quadrant small well defined smooth margin oval-shaped lesion, show low SI on TW2, high SI on STIR, restricted diffusion (high SI on DWI and low SI on ADC), rim enhancement, type III malignant (washout) curve, pathologically proved TNBC, ILC.

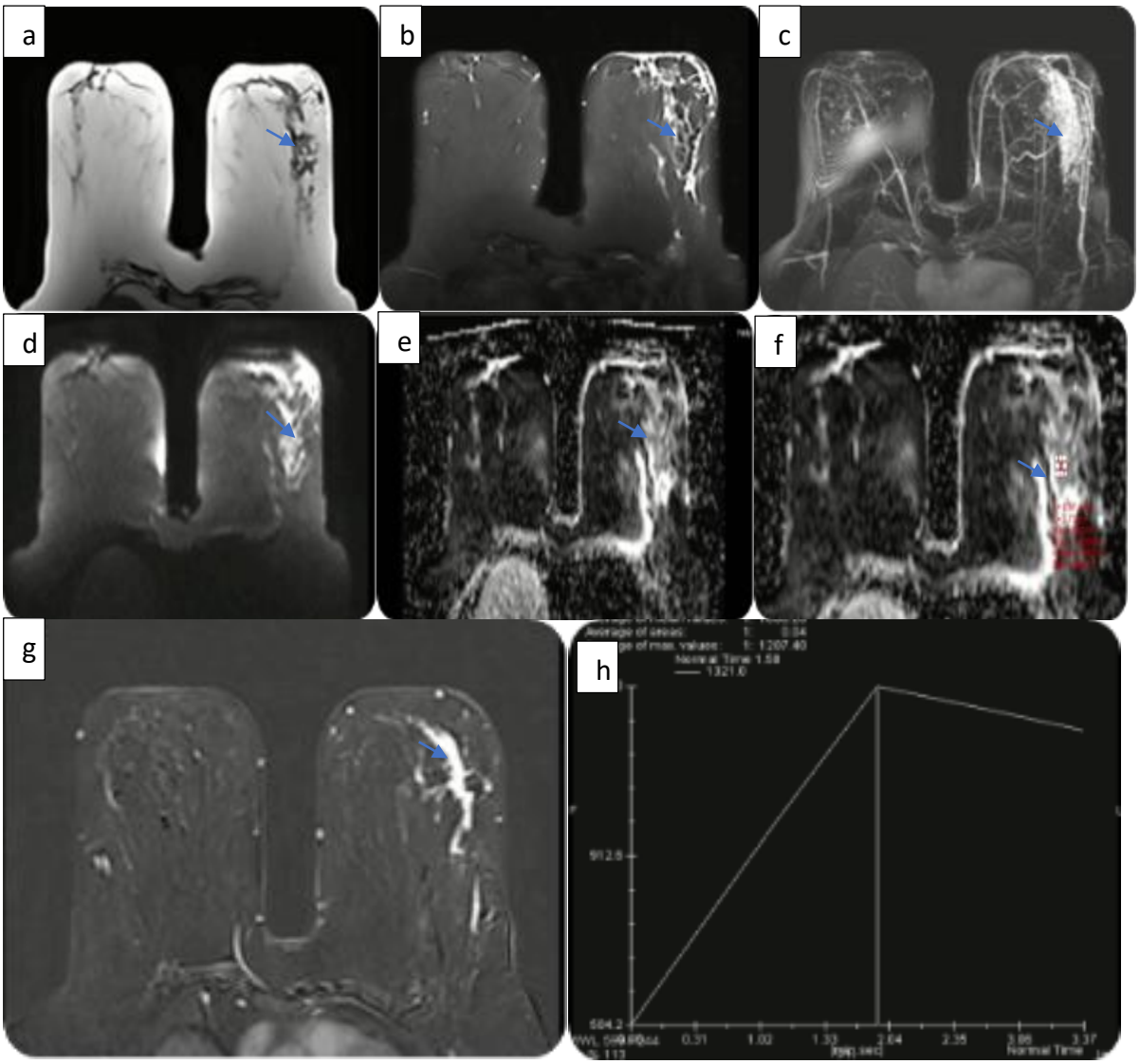

Fig. (3): Female patient 53 years old age, came for screening, a) T2WI, b) STIR, c)MIP, d)DWI, e)ADC map, f)ADC value, g) DCE-MRI subtracted postcontrast series & h) Dynamic curve (arrows) revealed Left-sided breast upper outer quadrant segmental like lesion displaying hypointense on T2WI, hyperintense on STIR, restricted diffusion(high SI on DWI & low on ADC), ADC value(1.05 X $10^{-3}mm^2/S$), non-mass enhancement of segmental distribution, type III (malignant) washout curve, pathologically proved to NTNBC, IDC.

DISCUSSION

Unfortunately, routine breast imaging procedures like ultrasound and mammography lack the typical malignant characteristics in TNBC subtype lesions. Additionally, because of the smaller sample size or the presence of heterogeneous tumor status, an Excisional biopsy is more trustworthy than a core needle biopsy[7].

Therefore, the presence of certain TNBC imaging characteristics may help with prognosis and pretreatment planning. Malignant characteristics were more pronounced on DCE-MRI than on conventional imaging, and it can be used to diagnose this cancer subtype [8].

Understanding the unique imaging characteristics of TNBC is crucial, which is why our study's goal is to emphasize these characteristics in comparison to other NTBC subtypes.

Based on immunochemistry data, all 83 pathologically confirmed malignant breast lesions in our current retrospective investigation, which included 68 female patients, were divided into two subtype groups: TNBC subtype group (22 patients/29 lesions) and NTNBC subtype group (46 patients/54 lesions).

According to **Azzam *et al.*** [9] whose patients ranged in age from 24 to 60 years (mean age 44 ±.04 SD), our observation that patients with the TNBC subtype were younger than other NTNBC patients with (mean age 41±1.3 Vs 52±2.4, p =0.0001) agreed with other researches [10,11].

Invasive ductal carcinomas were the most prevalent histological subtype in both groups of patients (IDC), representing (58.6%) for TNBC Vs (50%) for NTNBC subtypes. However, **Moffa *et al.*** [7]**,** noted that there were no admixtures of other cancer types in TNBCs; this discrepancy across the studies may be due

to the fact that TNBC develops quickly and is therefore often misdiagnosed as a different disease[12].

Although it has been suggested that TNBC is associated with a higher rate of lymph node positivity [8], in our study there was no difference in the rate of lymph node positivity between the two subtypes (P=0.337).

According to **Garry *et al.* [13],** unifocal lesions and TNBC were strongly associated. In our analysis, multifocality was only observed in 6.9% of TNBC as opposed to (1.9%) in NTNBC, with a p-value of 0.850436.

With an average tumor size of 2.7 to 4.1 cm, TNBC tumor size is typically greater than non-TNBC on MRI upon diagnosis [7,8,13]. Also, according to **Moffa *et al.* [7]**, reported that almost 60% of TNBCs measured >2 cm, this agreed with our results where, larger tumors (>2 cm) predominated in the TNBC subtype compared to NTNBC (72.4% Vs 42.6%, P=0.05).

Our results were consistent with those of several earlier studies [13,14,15] that demonstrated that the majority of TNBC lesions presented as an enhancing mass with a round or oval form. However, **Sung *et al.* [16]** observed that the majority of TNBC lesions were lobulated.

In terms of the lesion margin, smooth margins were more noticeable in TNBC lesions than in NTNBC lesions (74.4 Vs 12.9%, P 0.00001), which was consistent with earlier studies [8,14,17], but different from other studies (9,13), where most masses had irregular or speculated margins (72/104, 69.2%), and (47% and 41%), respectively.

Our results showed that TNBC had significantly higher rates of intra-tumoral high T2 signal intensity compared to NTNBC on unenhanced fat-suppressed T2-weighted images (79.3% vs 27.8%, p=0.00001). This finding was in line with numerous previous studies [9,14,16] showing that high intra-tumoral T2 signal intensity is strongly associated with TNBC.

In our study, the TNBC subtype restricted diffusion was more pronounced than the NTNBC subtype (65.5% Vs 31.5%). This outcome was lower than the previous study's DWI's 92.5% cancer detection rate [7]. Furthermore, our study's tumor subtypes showed significantly different detectability at DWI, with a p-value of 0.002853, in contrast to **Youk *et al.* [8]** findings that their tumor subtypes showed no significant variation in detectability at DWI (P=0.911).

According to **Tianwen *et al.* [18],** TNBC had greater ADC values than other subtypes. Our findings showed that ADC values were significantly higher at TNBC subtypes & different among two tumor subtypes with P value= 0.0412 were in agreement with **Youk *et al.* [8]** findings that ADC value was significantly different among tumor subtypes (P 0.0001) and significantly correlated with TNBC (P 0.002). One explanation for this finding is that TNBC was more frequently associated with intra-tumoral necrosis tumor cellularity can decrease in necrotic parts [19, 20].

The presence of strong angiogenesis in the tumor's periphery, core necrosis, or fibrosis can all be used to explain rim enhancement [7]. In this investigation, 58.6% of TNBCs were characterized as having internal enhancement features that were rim enhancement, compared to reports of 80% by **Uematsu *et al.* [17],** 76% by **Dogan *et al.* [21],** 68% by **Angelini *et al.* [22], and** 57% by **Sung *et al.* [16].**

This result is like many studies [2,8,9,23] which documented that most of the patients in their study showed borderline and malignant pattern kinetic curves (types II and III), in contrast to **Uematsu *et al.* [17],** who reported that a persistent enhancement pattern was significantly associated with TNBC. Instead, we found that type III (wash-out) and type II (plateau) curves in (16/29,55.2%), and (10/29,34.5%) of TNBC.

According to the previous study [24] and this study, the occurrence of intralesional necrosis was the other positive predictor of the TNBC subtype [17]. We observed a highly significant difference between TNBC and NTNBC regarding the central necrosis detection rates (11/29,37.9% Vs 4/54,7.4%, p=0.05).

Peritumoral edema, another characteristic of breast tumors visible on T2-weighted sequences, is correlated with the biologically aggressive TNBC subtype [25, 26]. In contrast to **Moffa *et al.* [7],** findings that there was no correlation between TNBC and peritumoral edema, perilesional edema was discovered in our study in 15/29, 51.7% of TNBCs versus 11/24, 20.4% of NTNBC, with a statistically significant difference (p=0.05). This discrepancy may be due to the larger tumor size in our study as compared to theirs.

Sensitivity%, specificity%, positive predictive value (PPV), and negative predictive value (NPP) of combined DCE-MRI and MRI-Specific criteria in differentiating between TNBC & NTNBC subtypes were (100%, 91.49%, 87.1% 100%) versus (88.89%, 97.87%, 96%, and 93.9%), respectively. Similar results were reported by **Schmadeka *et al.* [11]** who suggested that MRI is the most sensitive (99–100%) imaging modality in the diagnosis of TNBC.

Our research has some limitations. First, it was a monocentric retrospective study with a small number of patients, the findings need to be confirmed in prospective studies with a broader sample. Second, MRI breast assessment can be subjective. This was mitigated by incorporating two or more experienced readers to reach a consensus.

CONCLUSION

TNBC typically affects young women and has a variety of MRI-based distinctive features, such as a rim-enhancing mass with an oval or round shape and a smooth border, central necrosis, and peri-tumoral edema, all of which favors TN breast cancer over non-TN breast cancer. It might be caused by the TN breast

cancer's aggressive histologic behavior. In patients with triple-negative and non-triple-negative breast cancer, MRI findings may be useful for organizing the course of treatment and determining prognosis.

Abbreviations

TNBC: Triple negative breast cancer; DCE-MRI: Dynamic contrast enhanced magnetic resonance imaging; NTNBC: Nontriple negative breast cancer; ADC: Apparent diffusion coefficient; T2WI: T2 relaxtion time weighted imaging; HER2: Human epidermal growth factor receptors 2; NCT: Neoadjuvent chemotherapy ; BI-RADS: Breast imaging reporting and data system; T1WI: T1 relaxtion time weighted imaging; DWI: Diffusion-weighted imaging; FSE: Fat spin echo; TR: Repitition time ;TE :Time to echo ; FOV: Field of view ; STIR :Short tau inversion recovery ;GRE: Gradient recalled ;MIP :Maximum intensity projection ;NPV: Negative Predictive value; PPV: Positive predictive value ; IDC:Intraductal carcinoma ;ILC :Intralobular carcinoma.

Financial support and sponsorship: Nil.

Conflict of interest: Nil.

REFERENCES

1. **Harada T, Uematsu T, Nakashima K *et al.* (2020):** Is the presence of edema and necrosis on T2WI pretreatment breast MRI the key to predict PCR of triple-negative breast cancer? Eur Radiol., 30: 3363–3370.
2. **Li Y, Chen Y, Zhao R *et al.* (2022):** Development and validation of a nomogram based on pretreatment dynamic contrast-enhanced MRI for the prediction of pathologic response after neoadjuvant chemotherapy for triple-negative breast cancer. Eur Radiol., 32: 1676–1687.
3. **Feng Q, Hu Q, Liu Y *et al.* (2020):** Diagnosis of triple-negative breast cancer based on radionics signatures extracted from preoperative contrast-enhanced chest computed tomography. BMC Cancer, 20: 579-84.
4. **Dogan B, Turnbull L (2012):** Imaging of triple-negative breast cancer. Annals of Oncology, 23(6):23-vi29.
5. **Bae M, Shin S, Ryu H *et al.* (2016)**: Pretreatment MR imaging features of triple-negative breast cancer: association with response to neoadjuvant chemotherapy and recurrence-free survival. Radiology, 281(2):392–400.
6. **Abdel Hafez A, Musall B, Hess K *et al.* (2021):** Tumor necrosis by pretreatment breast MRI: association with neoadjuvant systemic therapy (NAST) response in triple-negative breast cancer (TNBC). Breast Cancer Res Treat., 185: 1–12.
7. **Moffa G, Galati F, Collalunga E *et al.* (2020):** Can MRI Biomarkers Predict Triple-Negative Breast Cancer? Diagnostics (Basel), 10(12):1090-95.
8. **Youk J, Son E, Hess K *et al.* (2012):** Triple-negative invasive breast cancer on dynamic contrast-enhanced and diffusion-weighted MR imaging: comparison with other breast cancer subtypes. Eur Radiol., 22: 1724–1734.
9. **Azzam H, Kamal R, El-Assaly H *et al.* (2020):** The value of dynamic contrast-enhanced MRI in the diagnosis and management of triple-negative breast cancer. Egypt J Radiol Nucl Med., 51: 1-6.
10. **Li J, Han X (2014):** Research and progress in magnetic resonance imaging of triple-negative breast cancer. Magnetic Resonance Imaging, 32(4):392–396.
11. **Schmadeka R, Harmon B, Singh M (2014):** Triple-negative breast carcinoma current and emerging concepts. Am J Clin Pathol., 141(4):462–477.
12. **Kumar P, Aggarwal R (2016):** An overview of triple-negative breast cancer. Arch Gynecol Obstet., 293:247–269.
13. **McGarry W, Bhole S (2018):** Triple-Negative Breast Cancer: What Crucial Information Can Imaging Add to the Diagnosis, Treatment, and Prognosis? Int J Women's Health Wellness, 5: 87-91.
14. **Osman N, Chalabi N, Abd Raboh N (2014):** NM Triple-negative breast cancer: MRI features in comparison to other breast cancer subtypes with correlation to prognostic pathologic factors. Egypt J Radiol Nucl Med., 45(4):1309–1316
15. **Ivanac G, Dominkovic M, Brkljacic B (2014):** Imaging features of triple-negative breast carcinoma: mammography, ultrasound, and MRI. European Society of Radiology. ECR., 2: C-0482. https://dx.doi.org/10.1594/ecr2014/C-0482
16. **Sung J, Jochelson M, Brennan S *et al.* (2013):** MR imaging features of triple-negative breast cancers. The Breast J., 19(6):643–649.
17. **Uematsu T, Kasami M, Yuen S (2009):** Triple-negative breast cancer: correlation between MR imaging and pathological findings. Radiology, 250(3):638–647
18. **Tianwen X, Qiufeng Z, Caixia F (2019):** Differentiation of triple-negative breast cancer from other subtypes through whole-tumor histogram analysis on multiparametric MR imaging. European Radiology, 29:2535–2544
19. **Padhani A, Liu G, Koh D *et al.* (2009):** Diffusion-weighted magnetic resonance imaging as a cancer biomarker: consensus and rec- commendations. Neoplasia, 11:102–125.
20. **Park S, Moon W, Cho N *et al.* (2010):** Diffusion-weighted MR imaging: pretreatment prediction of response to neoadjuvant Chemotherapy in patients with breast cancer. Radiology, 257:56–6.
21. **Dogan B, Gonzalez-Angulo A, Gilcrease M (2010):** Multimodality imaging of triple receptor-negative tumors with mammography, ultrasound, and MRI. AJR Am J Roentgenol., 194:1160–1166.
22. **Angelini G, Marini C, Iacconi C (2018):** Magnetic resonance (MR) features in triple-negative breast cancer (TNBC) vs receptor-positive cancer (nTNBC) Clin. Imaging, 49:12–16.
23. **Chen J, Agrawal G, Feig B (2007):** Triple-negative breast cancer: MRI features in 29 patients. Ann Oncol., 18:2042–2043.
24. **Gigli S, Amabile M, David E (2019):** De Luca A, Grippo C, Manganaro L, Monti M, Ballesio L. Morphological and semiquantitative kinetic analysis on dynamic contrast-enhanced MRI in triple-negative breast cancer patients. Acad Radiol., 26:620–625.
25. **Panzironi G, Moffa G, Galati F (2020):** Peritumoral edema as a biomarker of the aggressiveness of breast cancer: Results of a retrospective study on a 3 T scanner. Breast Cancer Res Treat., 181:53–60.
26. **Costantini M, Belli P, Distefano D (2012)**: Magnetic resonance imaging features in triple-negative breast cancer: Comparison with luminal and HER2-overexpressing tumors. Clin Breast Cancer, 12:331–339.